

Soft-Switched Synchronous Buck Converter for Battery Chargers

Zhiyong Dong^{1*}, and Gyubum Joung¹

^{1*}PhD student, ¹Professor, Energy and Electrical Engineering, Woosuk University, Korea
^{1*}120112296@stu.woosuk.ac.kr, ¹gbjoung@woosuk.ac.kr

Abstract

In this paper, we proposed a soft-switched synchronous buck converter, which can perform charging the battery. The proposed converter has low switching loss even at high frequency operation due to its soft switching characteristics. The converter operates in synchronous mode to minimize conduction loss, resulting in small conduction loss, also. In this reason, the efficiency of the converter can be greatly improved even in high frequency. The size and weight of the converter can be reduced by high frequency operation of the converter. In this paper, we designed a battery charger with a switching frequency of 100 kHz. The designed converter also simulated to prove the converter's characteristics of synchronous operation as well as soft switching operation. The simulation shows that the proposed converter always meets the soft switching conditions of turning on and off switching in the zero voltage and zero current states. Therefore, simulation results have confirmed that the proposed battery charger had soft switching characteristics. The simulation results for transient response to charge current for the designed converter show that the converter responds to charge current commands quickly within 0.05 ms.

Keywords: Soft switched converter, Synchronous converter, Low switching loss, Battery charger.

1. Introduction

Converters used in industry have mostly used pulse width modulation (PWM) converters [1] [2]. In the case of moving objects such as cars, satellites, and aircraft, the converters need to minimize weight and volume. Minimizing the weight and volume of the converters requires minimizing filters with inductors, capacitors, which make up the bulk of the weight and volume. These require that the converter must operate at a high switching frequency. Therefore, resonant converters have commonly used for high frequency operation. [3] [4] However resonant converters generally have low switching losses but have a disadvantage of increased conduction losses. [5] [6] Many researches have been researched the converters of the soft switched PWM converters to reduce conduction loss of the resonant converter. In order to maximize the efficiency of the converter by reducing the conduction loss of the diode, research have been actively conducted on a soft switched synchronous PWM converter. [7] [8]

In this study, we proposed a soft switched synchronous buck converter. The proposed soft switched

synchronous buck converter has the characteristics of very low switching loss because of its soft switching characteristics. Also, the conduction loss has much reduced by synchronous operation of the converter. Therefore, the switching loss and conduction loss can be very low even in the high frequency operation of the converter, which has the characteristics of high efficiency. The size and weight is minimized by high frequency switching operation of the converter. In this paper, the soft switched proposed converter for battery charger has analyzed, designed, and simulated by piecewise linear electrical circuit simulation (PLECS) software. The simulation confirmed that the proposed battery charger had soft switching and synchronous characteristics during operation. We also simulated the transient response of the designed converter. The results show that the converter responds to charge current commands quickly within 0.05 ms.

2. Proposed Converter

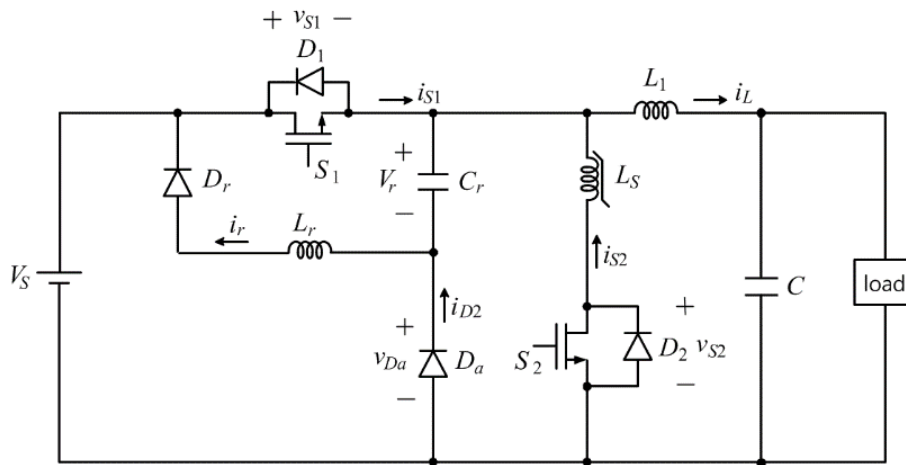


Figure 1. Proposed buck converter

Figure 1 shows a proposed converter, in which the switches of the converter are switched at zero current or zero voltage and the converter operates in synchronous mode. In Figure 1, the inductance of saturable inductor L_S is L_{S2} when the inductor is saturated and L_{S1} when the inductor is not saturated. The saturation current of inductor L_S is assumed as I_{L_S} . Figure 2 shows the voltage and current waveforms of the main components of the converter according the switching operation of the proposed converter in Figure. 1. As shown in Figure 2. The switch S_1 and S_2 operates at soft switching conditions. In Figure.2, the waveforms represents the switch S_2 is turn off at zero current, and the switch S_2 turn on at zero voltage and zero current. The switch S_1 is turn on at zero current and turn off at low voltage. Synchronous operation of S_2 can be realized by turning on S_2 as soon as D_2 is turn on.

Figure 3 is the operating modes of the proposed converter. The operating modes of the converter according to the switching S_1 , S_2 is composed of seven modes. The converter's operating conditions and analysis results for each mode in Figure 3 are as follows. Where, it is assumed that the current i_L and the output voltage v_o are constant I_L and V_o , respectively, during the switching period. In addition, the angular resonant frequency ω and characteristic impedance Z of the resonant circuit are as follows.

$$\omega = \frac{1}{\sqrt{L_r C_r}} \tag{1}$$

$$Z = \sqrt{\frac{L_r}{C_r}} \tag{2}$$

In Eq.(1) and (2), L_r is the resonant inductance and C_r is the resonant capacitance in Figure 1.

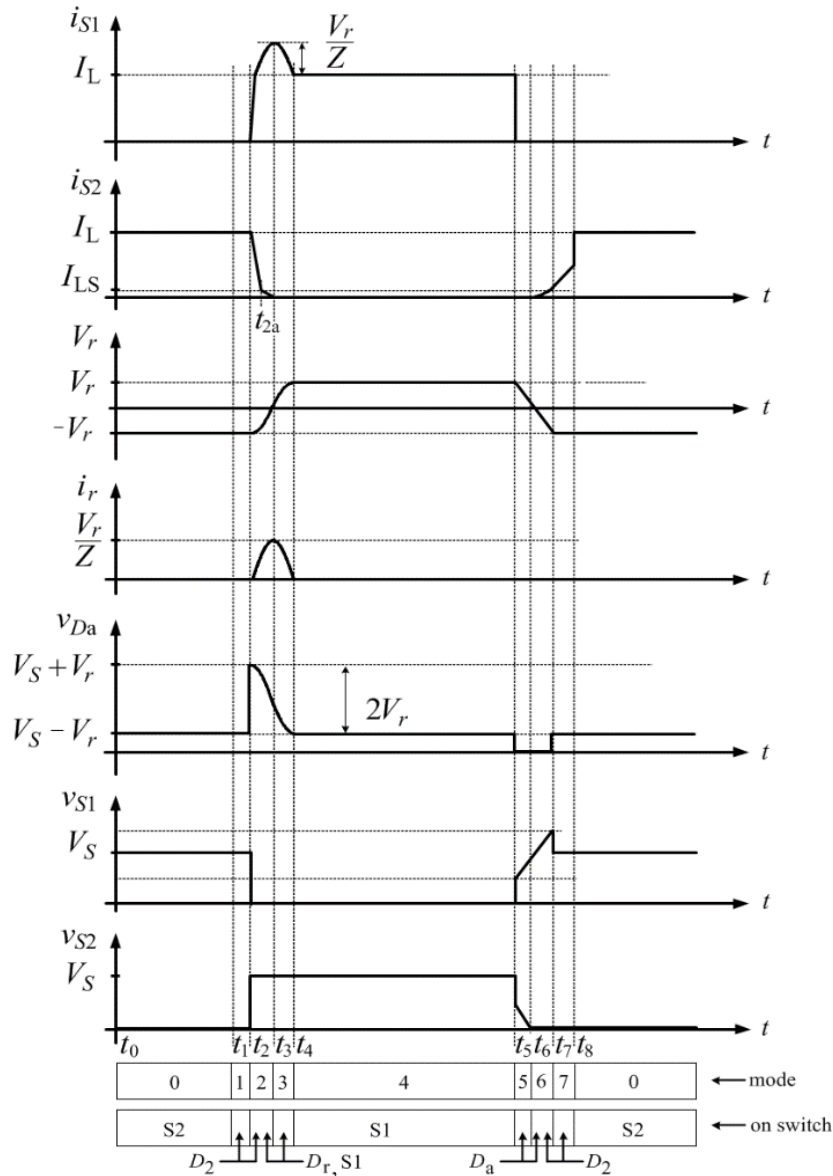


Figure 2. Switching waveforms of proposed converter

Mode 0 ($t_0 \leq t \leq t_1$)

When the switch S_2 turns on to realize synchronous operation and all other switches remain off at t_0 , the converter operates in mode 0 as shown in Figure 3(a). Therefore, the voltage and current waveforms of each element of the converter are shown in Fig. 2 (a). Where, the voltage v_r of capacitor C_r is determined in mode 6 and the initial v_r is assumed to be $-V_r$.

Mode 1 ($t_1 \leq t \leq t_2$)

Mode 1 starts when the switch S_2 turns off. When switch S_2 is off, the current i_L in inductor L flows through diode D_2 , so the converter operates in mode 1 of Figure 3 (b). Since diode D_2 is on instead of switch S_2 , the voltage and current waveforms of each element of the converter are the same waveforms as shown in Figure 2.

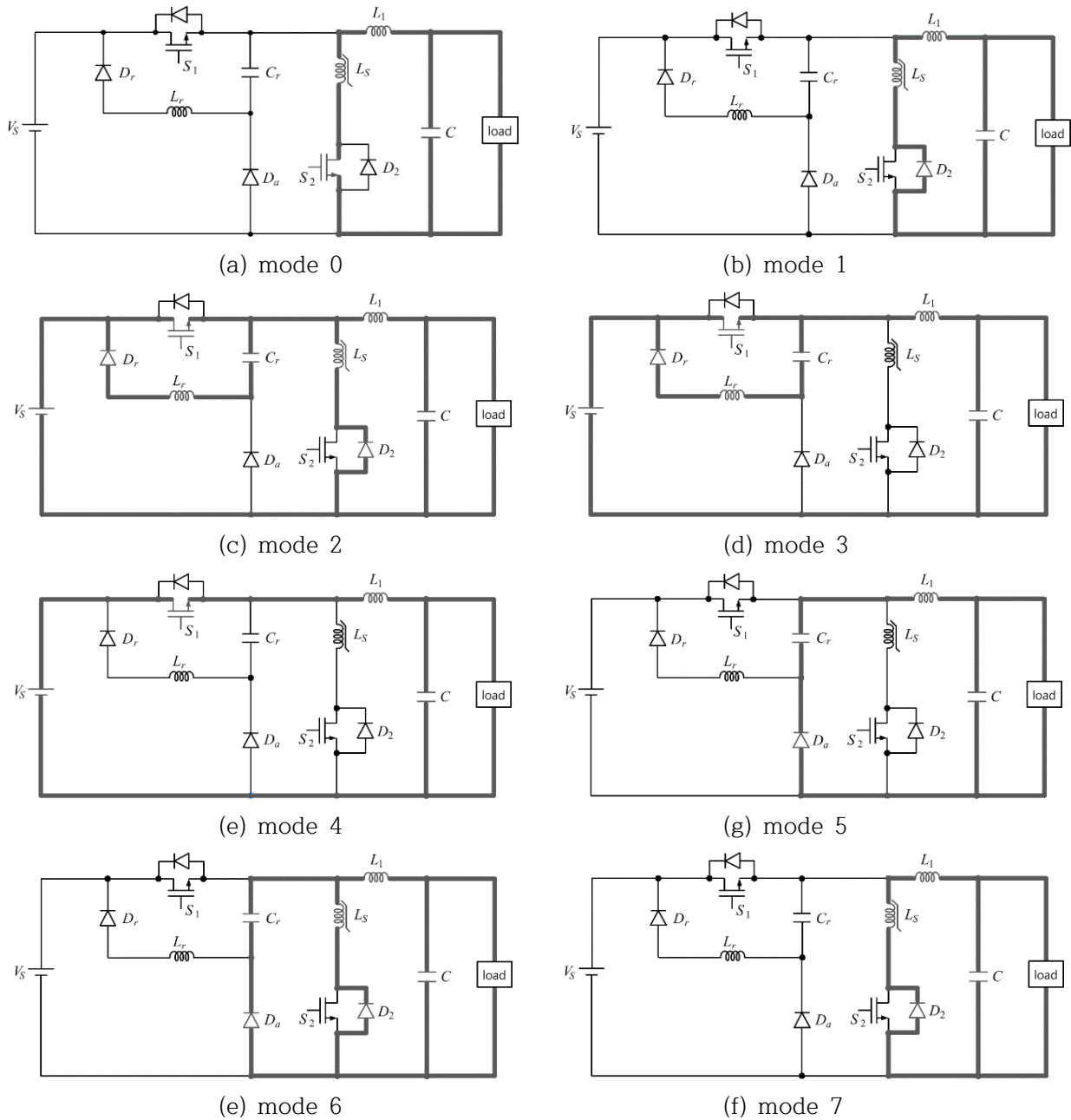


Figure 3. Operating modes of the proposed converter

Mode 2 ($t_2 \leq t \leq t_3$)

Mode 2 starts when switch S_1 turns on. When S_1 is on state, the converter operates in mode 2 of Figure 3(c). As shown in Figure 3(c), the voltage V_S is applied across the saturable L_S . Therefore, the inductor current i_{S2} is

$$i_{s2} = I_L - \frac{V_S}{L_{S1}}(t - t_1) \quad (t_2 \leq t \leq t_{2a}) \quad (3)$$

Where $i_{s2}(t_{1a}) = I_{LS}$

When the saturable inductor L_S is unsaturated at t_{2a} , the inductance is changed from L_{S1} to L_{S2} . Therefore, i_{s2} is

$$i_{s2} = I_{LS} - \frac{V_S}{L_{S2}}(t - t_{2a}) \quad (t_{2a} \leq t \leq t_3) \quad (4)$$

The current i_{s2} becomes zero at t_3 in Eq. (4), and mode 2 ends at t_3 .

When mode 2 starts at t_2 , the resonant circuit ($S_1 - C_r - L_r - D_r$) operates as shown in Fig. 3 (c), and the inductor current i_r and capacitor voltage v_r are analyzed as follows.

$$i_r = \frac{V_r}{Z} \sin[\omega_r(t - t_2)] \quad (5)$$

$$v_r = -V_r \cos[\omega_r(t - t_2)] \quad (6)$$

In Eq.(5) and (6), V_r is the initial voltage v_r . The maximum voltage of v_r is limited to V_S .

Mode 3 ($t_3 \leq t \leq t_4$)

Even if the current i_{s2} becomes zero and mode 2 finishes, the resonant circuit continues to operate as shown in Figure 3(c). The current i_r and voltage v_r are the same as in Eq.(5) and Eq.(6). Mode 3 finishes when the resonant current i_r becomes zero. At the end of mode 3, the capacitor voltage $v_r(t_4)$ is V_r .

Mode 4 ($t_4 \leq t \leq t_5$)

When the resonant current i_r reaches zero in mode 3, only MOSFET S_1 is turned on as shown in Figure 1, and mode 4 starts. Mode 4 continues until MOSFET S_1 is turned off.

Mode 5 ($t_5 \leq t \leq t_6$)

When the switch S_1 is turned off at t_5 , the mode 4 starts. Since the capacitor voltage v_r is less than zero, the inductor current i_r flows through the capacitor C_r as shown in Figure 3 (f). Therefore, the capacitor voltage v_r is reduced as follows.

$$v_r = V_r - \frac{I_L}{C_r} t \quad (7)$$

Mode 6 ($t_6 \leq t \leq t_7$)

When the capacitor voltage v_r reaches 0 V, diode D_2 begins to turn on, and the current i_{s2} of the saturable inductor gradually increases as shown in Figure 2. As the current i_{s2} slowly increases to I_L , the diode D_a naturally turns off. At the end of mode 6, the capacitor voltage v_r is $-V_r$. The voltage V_r depends on the charging current I_L .

Mode 7 ($t_7 \leq t \leq t_8$)

When $i_{s2} = I_L$ in mode 6, the diode D_a turns off naturally, the circuit operates at mode 7 as shown in Figure 3(h). To maximize synchronous operation period, the mode 7 reduces as shot as possible.

Table 1. Switch S_1 , S_2 Operating mode

		Switching Operations
S_1	on \rightarrow off	ZVS (Zero Voltage Switching) in high charging current Partially hard switching in low charging current
	off \rightarrow on	ZCS (Zero Current Switching)
S_2	on \rightarrow off	ZCS
	off \rightarrow on	ZVS / ZCS

Table 1 shows the summary of the switching states for switches S_1 and S_2 . From Table 1, we can see that the switches S_1 and S_2 always perform soft switching operation.

3. Simulations results

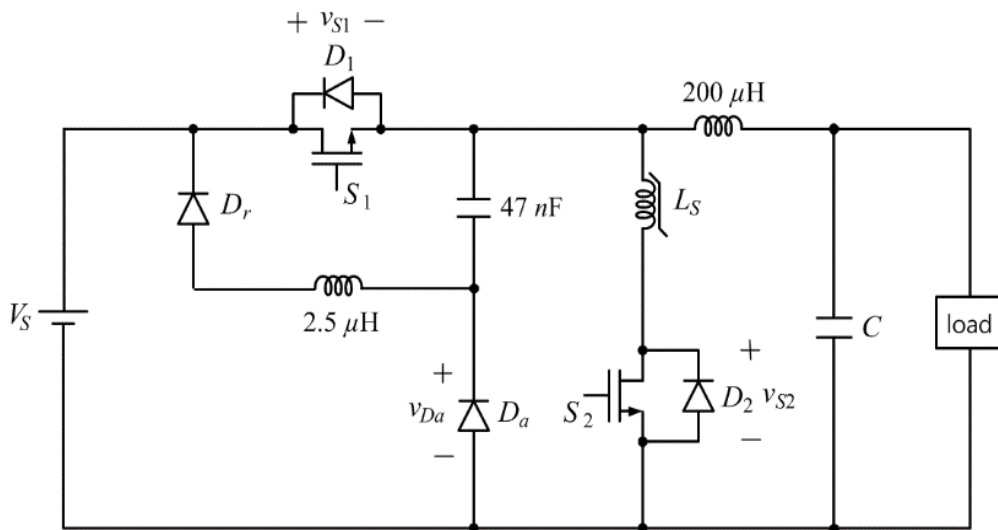


Figure 4. Deigned Battery Charger Circuit for simulation

The circuit as shown in Figure 4 was simulated used a PLECS simulation program. In the circuit, V_S is 48 V, the load is 32 V, which is the voltage of the battery. In Figure 4, the battery current is the average of the inductor current, and the simulation controller has designed to control the battery charge current.

Figure 5 shows the voltage and current waveforms of the charger circuit elements when the battery charge current is 5A. In Figures 5, the voltages and currents of the components of the charger circuit are similar to the waveforms in Figure 2. From the waveforms in Figures 5, the MOSFETs and diodes in the circuit show mostly soft switching operation when turned on and turn off. From the voltage waveform of switch S_1 in Figure 5, the MOSFET shows partially hard switching when it has turned off.

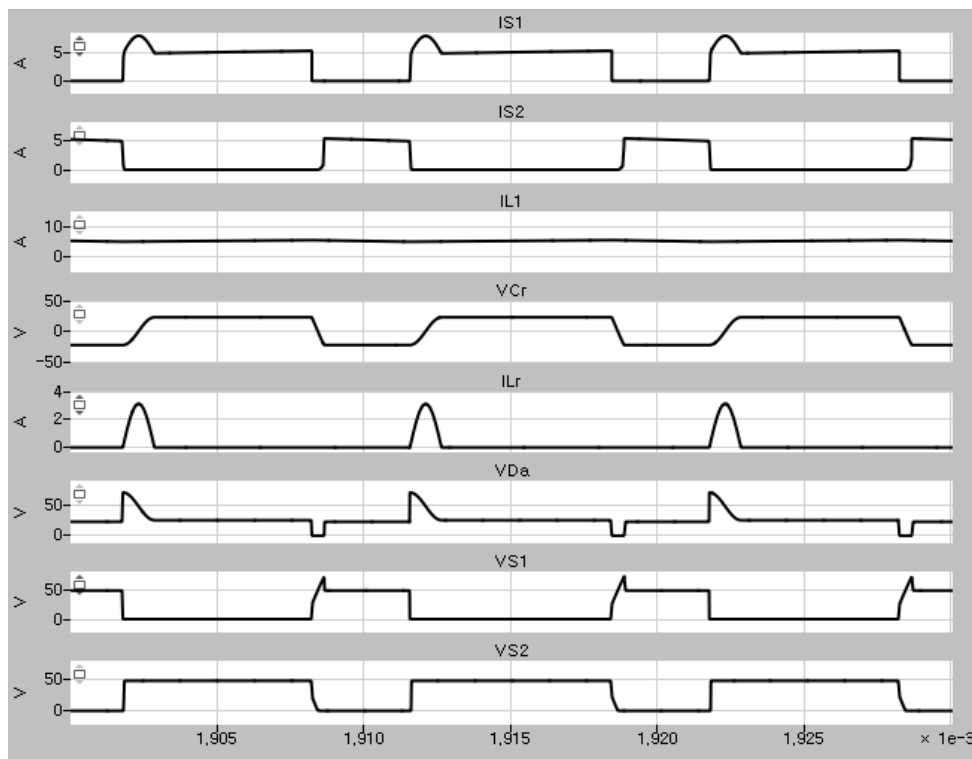


Figure 5. Voltage and current waveforms of battery charger circuit

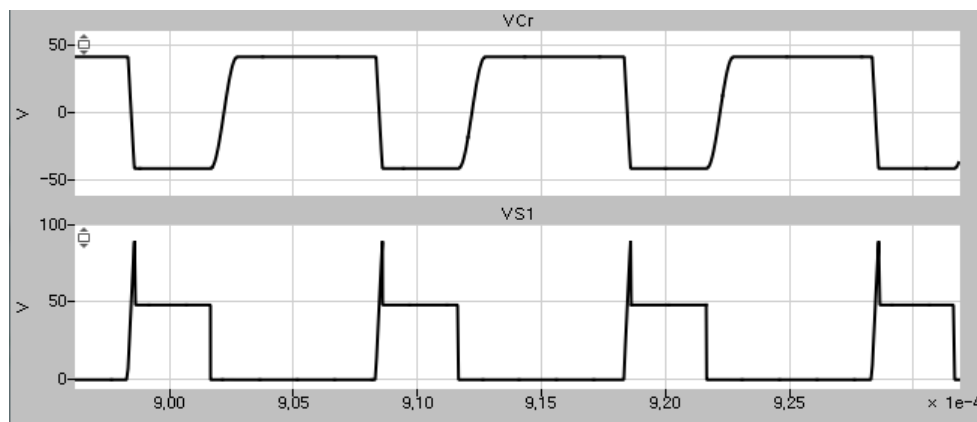


Figure 6. Voltage waveforms of V_{S1} , V_{cr} for battery charger circuit

Figure 6 shows the voltage waveforms of capacitor voltage and MOSFET S_1 when the battery charge current is 15 A. As battery charging current increases, the energy of saturable inductance L_{S1} increases, the initial resonant capacitor voltage $v_r(t_0)$ is limited to input voltage V_S . Therefore, the MOSFET S_1 is soft switching when it has turned off as shown in Figure 6.

Figure 7 is the transient response of the designed converter for changing battery charging current. As shown in Figure 7, changing the controller's battery charge current command quickly controls the inductor current I_L to within 0.05 ms.

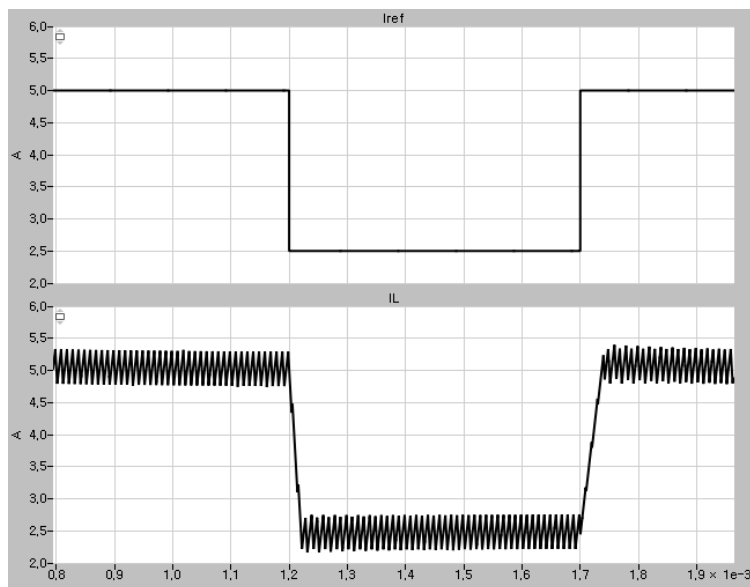


Figure 7. Transient results (I_{REF} : battery reference command, i_L : inductor current)

4. Conclusions

In this study, we proposed a soft switched synchronous buck converter. The proposed converter has the characteristics of very low switching loss because of its soft switching characteristics. The conduction loss has much reduced by synchronous operation of the converter, also. Therefore, the switching loss and conduction loss can be very low even in the high frequency operation of the converter, which has the characteristics of high efficiency. By high frequency operation, the compact design of the converter can be possible. In this paper, the soft switched proposed converter for battery charger has analyzed, designed, and simulated by PLECS. The simulation confirmed that the proposed battery charger had soft switching and synchronous characteristics.

Acknowledgement

This research was supported by the Ministry of Trade, Industry & Energy (MOTIE), Korea Agency for Technology and Standards (KATS) for Standard Program – 20006875

References

- [1] S. Thongkullaphat, "Improved Charge Pump Power Factor Correction Electronic Ballast Based on Class DE Inverter," *Internal Journal of Advanced Smart Convergence*, vol. 4, no. 1, pp. 64-70, May, 2015.
- [2] B.G. Kim, K.W. Kim, T.S. Jang, J.M. Lee, and Y.K. Kim, "Development of Current Control System for Solar LED Street Light System," *Internal Journal of Advanced Smart Convergence*, vol. 1, no. 1, pp. 52-56, May, 2012.
- [3] J.M. Kwon, W.Y. Choi, and B.H. Kwon, "Single-Switch Quasi-Resonant Converter," *IEEE Trans. on Industrial Electronics*, vol. 56, no. 4, pp. 1158-1163, April, 2009.
- [4] G.B. Joung, C.T. Rim, and G.H. Cho, "Integral cycle mode control of the series resonant converter," *IEEE Transactions on Power Electronics*, Vol. 4. No. 1, pp83-91, July, 1989.
- [5] M.R. Mohammadi and H. Farzanehfard, "New family of zero-voltage-transition PWM bidirectional converters with coupled inductors," *IEEE Trans. Ind. Electron.*, Vol. 59, No. 2, pp. 912-919, Feb. 2012

- [6] E. Adib and H. Farzanehfard, "Family of Zero-Current Transition PWM Converters, " *IEEE Trans. on Industrial Electronics*, vol. 55, no. 8, pp. 3055- 3063, August 2008.
- [7] S. Abedinpour, B. Bakkaloglu, and S. Kiaei, "A Multistage Interleaved Synchronous Buck Converter With Integrated Output Filter in 0.18 um SiGe Process," *IEEE Trans. Power Electronics*, vol.22, No. 6, pp. 2164–2175, Nov. 2007.
- [8] E. Adib and H. Farzanehfard, "Zero-Voltage-Transition PWM Converters With Synchronous Rectifier," *IEEE Trans. Power Electronics*, vol.25, No. 1, pp. 105–110, Jan. 2010.